Semiquinone Radicals from Oxygenated Polychlorinated Biphenyls: Electron Paramagnetic Resonance Studies

Yang Song, Brett A. Wagner, Hans-Joachim Lehmler, and Garry R. Buettner*

Department of Occupational and Environmental Health, Free Radical and Radiation Biology Program, and ESR Facility, The University of Iowa, The University of Iowa, Iowa City, Iowa 52242-1101

Received January 10, 2008

Polychlorinated biphenyls (PCBs) can be oxygenated to form very reactive hydroquinone and quinone products. A guiding hypothesis in the PCB research community is that some of the detrimental health effects of some PCBs are a consequence of these oxygenated forms undergoing one-electron oxidation or reduction, generating semiquinone radicals ($SQ^{\bullet-}$). These radicals can enter into a futile redox cycle resulting in the formation of reactive oxygen species, that is, superoxide and hydrogen peroxide. Here, we examine some of the properties and chemistry of these semiquinone free radicals. Using electron paramagnetic resonance (EPR) to detect $SQ^{\bullet-}$ formation, we observed that (i) xanthine oxidase can reduce quinone PCBs to the corresponding $SQ^{\bullet-}$; (ii) the heme-containing peroxidases (horseradish and lactoperoxidase) can oxidize hydroquinone PCBs to the corresponding $SQ^{\bullet-}$; (iii) tyrosinase acting on PCB *ortho*-hydroquinones leads to the formation of $SQ^{\bullet-}$; (iv) mixtures of PCB quinone and hydroquinone form $SQ^{\bullet-}$ via a comproportionation reaction; (v) $SQ^{\bullet-}$ are formed when hydroquinone-PCBs undergo autoxidation in high pH buffer ($\approx>$pH 8); and, surprisingly, (vi) quinone-PCBs in high pH buffer can also form $SQ^{\bullet-}$; (vii) these observations along with EPR suggest that hydroxide anion can add to the quinone ring; (viii) H_2O_2 in basic solution reacts rapidly with PCB-quinones; and (ix) at near-neutral pH SOD can catalyze the oxidization of PCB-hydroquinone to quinone, yielding H_2O_2. However, using 5,5-dimethylpyrroline-1-oxide (DMPO) as a spin-trapping agent, we did not trap superoxide, indicating that generation of superoxide from $SQ^{\bullet-}$ is not kinetically favorable. These observations demonstrate multiple routes for the formation of $SQ^{\bullet-}$ from PCB-quinones and hydroquinones. Our data also point to futile redox cycling as being one mechanism by which oxygenated PCBs can lead to the formation of reactive oxygen species, but this is most efficient in the presence of SOD.

Introduction

Polychlorinated biphenyls (PCBs) are a class of environmental pollutants that have from one to 10 chlorines substituted on the phenyl rings. PCBs have been widely used from the 1930s to the 1960s in diverse industrial applications, including cooling and insulating fluids for industrial transformers and capacitors, hydraulic fluids, and sealants (*1, 2*). PCBs are known to elicit various adverse effects, including carcinogenicity, neuroendocrine disturbances, developmental and reproductive toxicity, and immunotoxicity (*3, 4*). PCBs have been implicated in or related to cancer such as malignant melanoma, breast, and lung cancers in exposed populations (*5*). The production of PCBs was banned in the 1970s due to the high toxicity of most PCB congeners and mixtures. However, because of their physical and chemical properties, PCBs are quite stable; thus, they remain as ubiquitous environmental contaminants, which are frequently found as complex mixtures of isomers and congeners in air, water, soil, and dust on surfaces in homes and in factories (*6*).

Lower halogenated PCBs have been shown to be metabolized by rat microsomes to phenol and dihydroxybiphenyl metabolites (*7–9*). Robertson et al. have reported that the primary metabolites of 4-monochlorobiphenyl are 4′-chloro-2-hydroxybiphenyl, 4′-chloro-3-hydroxybiphenyl, and 4′-chloro-4-hydroxybiphenyl; these phenolic compounds can then subsequently undergo a second hydroxylation yielding 4′-chloro-3,4-dihydroxybiphenyl, 4′-chloro-2,3-dihydroxybiphenyl, and 4′-chloro-2,5-dihydroxybiphenyl (*10*). These *para*-dihydroxy PCBs and catechol type *ortho*-dihydroxy PCBs can be further oxidized to reactive quinones.

Early research suggests that the intracellular activation of hydroquinones and quinones producing relatively stable semiquinone free radicals is an important step to account for their cytotoxicity (*11*). Radicals produced "downstream", such as superoxide anion radical ($O_2^{\bullet-}$), will lead to hydrogen peroxide and hydroxyl radical formation ($HO^{\bullet}$); these active oxygen species will deplete antioxidants and potentially lead to an increase in oxidative stress (*12–15*). These reactive oxygen species can oxidize lipids, proteins, and DNA (*16–18*).

In the work reported here, we used EPR to examine the many routes that can lead to the formation of PCB-semiquinone radicals. We also examined the different spectral patterns of these various semiquinone radicals and used the changes observed in the EPR spectra to understand their chemistry.

Materials and Methods

Caution: *PCB derivatives should be handled as hazardous compounds in accordance with NIH guidelines.*

Materials. Hypoxanthine (HX),[1] xanthine oxidase (XO), horseradish peroxidase (HRP), tyrosinase (TYR), lactoperoxidase (LPO), catalase (Cat), superoxide dismutase (SOD), and diethylenetriaminepentaacetic acid (DETAPAC or DTPA) were from Sigma (St. Louis, MO); benzoquinone, hydroquinone, phenyl-quinone, sodium hydroxide, and H_2O_2 were from Fisher;

* To whom correspondence should be addressed. Tel: 319-335-6749. Fax: 319-335-9112. E-mail: garry-buettner@uiowa.edu.

10.1021/tx8000175 CCC: $40.75
Published on Web 06/13/2008

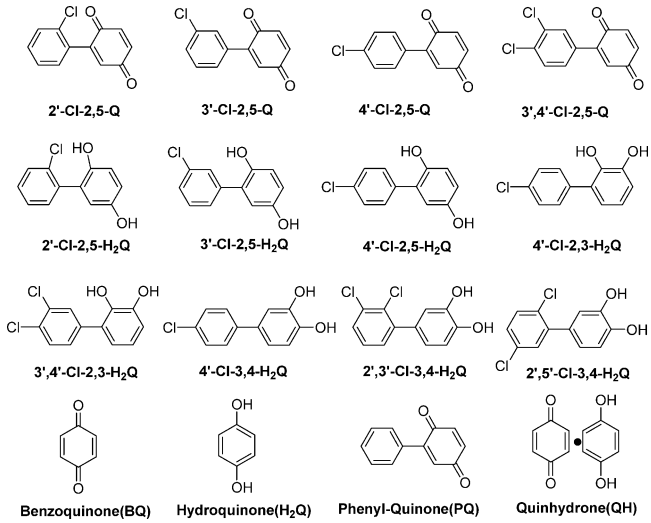

Figure 1. Chemical structures and nomenclature of the PCB quinones and hydroquinones used.

and quinhydrone was from Alfa Aesar (Ward Hill, MA). DMPO was from Dojindo Laboratories (Japan). Materials were used without further purification. The various PCB hydroquinones and quinones were synthesized as previously described (*19–21*). Stock solutions (200 mM each) of PCBs were prepared in DMSO. Stock solutions of HX (10 mM), HRP (0.2 U/μL), TYR (1 U/μL), H_2O_2 (20 mM), SOD (100 U/μL), and Cat (20 U/μL) were prepared with Nanopure water just before use; XO (10.8 mU/μL) and LPO (208 mU/μL) were used as received. All experiments were carried out in 100 mM phosphate buffer containing 250 μM DETAPAC. When needed, adjustment of the pH was done with 5 M sodium hydroxide solution. All of the PCB quinones and hydroquinones studied are shown in Figure 1.

EPR Spectroscopy. EPR spectroscopy was done using a Bruker EMX spectrometer equipped with a high-sensitivity cavity and an Aqua-X sample holder. Spectra were obtained at room temperature. Typical EPR parameters were as follows: 3511 G center field; 15 or 80 G sweep width (for the spin trapping experiments with DMPO); 9.854 GHz microwave frequency; 20 mW power; 2×10^5 receiver gain; modulation frequency of 100 kHz; modulation amplitude of 1 or 0.1 G; with the conversion time and time constant both being 40.96 ms with 5 X-scans for each 1024 point spectrum.

The final concentrations of PCB derivatives were 100 μM unless specifically mentioned. Alkaline solutions (pH 10) were prepared by adjusting with 5 M sodium hydroxide solution.

Spectral simulations of EPR spectra were performed using the WinSim program developed at the NIEHS by Duling (*22*). Correlation coefficients of simulated spectra were typically >0.99.

Oxygen Uptake. Oxygen uptake was determined with a Clark type electrode using an YSI model 5300 Biological Oxygen Monitor (Yellow Springs Instrument Co., Yellow Springs, OH). All measurements were made at room temperature; 3.00 mL of PBS buffer was loaded in the chamber of the oxygen monitor and aerated by stirring for 5 min, and then, the electrode was placed in contact with the solution, leaving no headspace for air and ensuring that all air bubbles were removed. After a 2 min equilibration, reagents were introduced through the access slot, and then, oxygen consumption was monitored. Each experiment was repeated at least three times. Results of replicate experiments varied less than $\pm 10\%$.

UV−Vis Spectroscopy. UV spectra were recorded with a Hewlett-Packard 8453 diode array spectrometer. All measurements were made at room temperature; 1.00 mL of PBS buffer was loaded in the cuvette, stirring with a small stirring bar to ensure that the solution mixed well. Using the kinetics setting, after the introduction of reagents, the change in absorbance at 249 nm was recorded vs time.

Scheme 1. Reaction Pathways of PCB Hydroquinone, Semiquinone, And Quinone[a]

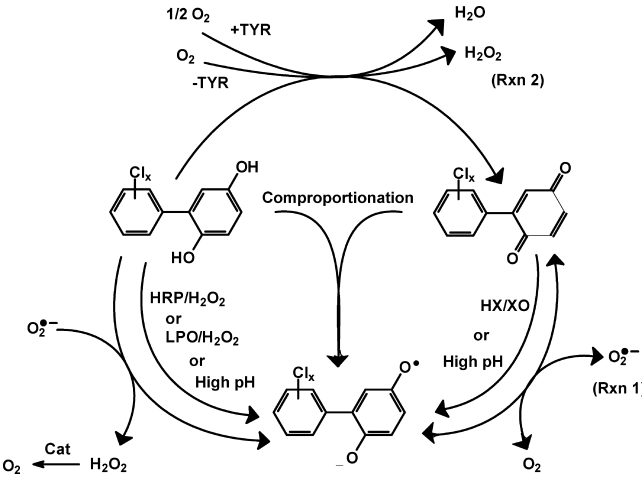

[a] High pH implies values greater than 8 or 9, as seen in Figure 7. Tyrosinase only acts on *ortho*-hydroquinones.

Results and Discussion

The generation of semiquinone radicals by oxidation/reduction of hydroquinones and quinones is well-documented (*23–25*). Polychlorinated biphenyls can be oxidized to hydroquinones (H_2Q) and quinones (Q). These species can be converted to their corresponding semiquinone free radicals ($SQ^{\bullet-}$) that will have a quite different reactivity than the parent quinone or hydroquinone. Here, we examine the formation of these $SQ^{\bullet-}$ radicals.

PCB Semiquinone Radicals Can Be Generated by Several Approaches. $SQ^{\bullet-}$ Via Xanthine Oxidase. The one-electron reduction of a quinone will yield its corresponding semiquinone radical. To determine if typical reducing enzymes can facilitate such a reaction, we examined the potential formation of $SQ^{\bullet-}$ from quinones by the molybdoflavin enzyme xanthine oxidase. Xanthine oxidase has been shown to reduce by one-electron compounds, such as adriamycin, to their corresponding $SQ^{\bullet-}$ (*26*) (Scheme 1). To demonstrate the usefulness of the hypoxanthine/xanthine oxidase system (HX/XO) in our experiments with PCB-derived quinones, we examined its ability to reduce 1,4-benzoquinone to its corresponding semiquinone radical. As seen in the EPR spectrum of Figure 2a, the well-studied five-line semiquinone free radical (1:4:6:4:1 intensity ratio, a^H (*4*) = 2.37 G) of 1,4-benzoquinone (*27, 28*) was obtained immediately after the introduction of 1,4-benzoquinone to the HX/XO enzyme system. This demonstrates the utility of HX/XO, a flavoenzyme, in studying the reductive formation of $SQ^{\bullet-}$ from Q.

[1] Abbreviations: a^H (4), hyperfine splitting constant due to four identical hydrogens; a^{H3}, hyperfine splitting due to the hydrogen on position 3 of the PCB phenyl ring; BQ, benzoquinone; Cat, catalase; DETAPAC, diethylenetriaminepentaacetic acid; DMPO, 5,5-dimethylpyrroline-1-oxide; H_2Q, hydroquinone; HRP, horseradish peroxidase; HX, hypoxanthine; LPO, lactoperoxidase; MnSOD, manganese-containing superoxide dismutase; PQ, phenyl-quinone; Q, quinone; QH, quinhydrone; SOD, superoxide dismutase; $SQ^{\bullet-}$, semiquinone; TYR, tyrosinase; x_n', represents a generic number of chlorines, each at a position n on the secondary ring; XO, xanthine oxidase.

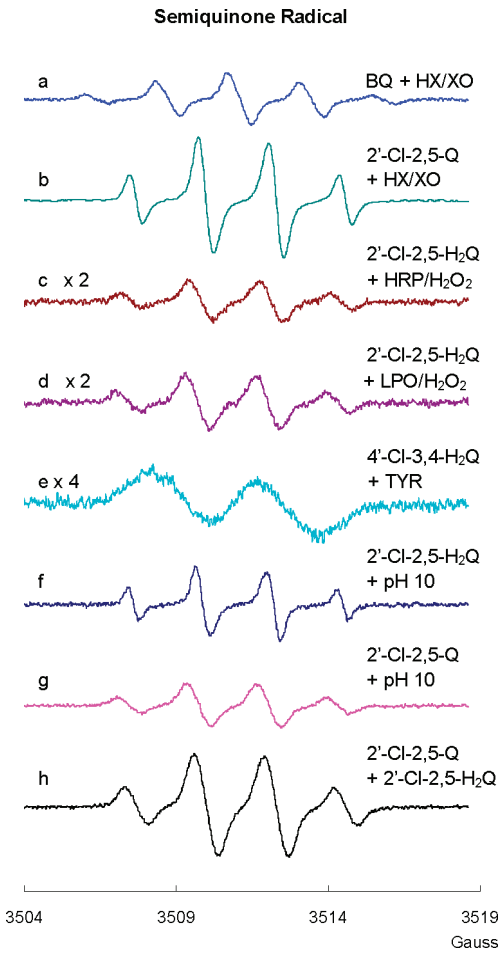

Figure 2. Semiquinone radical ($SQ^{\bullet -}$) can be formed by many routes: (a) $SQ^{\bullet -}$ generated from BQ reacted with HX/XO, [HX] = 50 μM, [XO] = 20 mU/mL; (b) $SQ^{\bullet -}$ generated from 2′-Cl-2,5-Q reacted with HX/XO, [HX] = 50 μM, [XO] = 20 mU/mL; (c) $SQ^{\bullet -}$ generated from 2′-Cl-2,5-H_2Q reacted with HRP/H_2O_2, [HRP] = 10 mU/mL, [H_2O_2] = 10 μM; (d) $SQ^{\bullet -}$ generated from 2′-Cl-2,5-H_2Q reacted with LPO/H_2O_2 system, [LPO] = 0.1 U/mL, [H_2O_2] = 10 μM; (e) $SQ^{\bullet -}$ generated from 4′-Cl-3,4-H_2Q reacted with tyrosinase, [TYR] = 2.5 U/mL; (f) $SQ^{\bullet -}$ generated from 2′-Cl-2,5-H_2Q at pH 10; (g) $SQ^{\bullet -}$ generated from 2′-Cl-2,5-Q at pH 10; and (h) $SQ^{\bullet -}$ generated from 2′-Cl-2,5-Q and 2′-Cl-2,5-H_2Q mixed 1:1, pH 7.4. The EPR modulation amplitude was 1 G for spectra a−e and h and 0.1 G for spectra f and g.

PCB-quinones can be viewed as substituted benzoquinone (Figure 1). Addition of the PCB-quinone 2′-Cl-2,5-Q to the HX/XO system (pH 7.4) resulted in a distinct four-line spectrum with $a^{H3} = a^{H4} = 2.1$ G and $a^{H6} = 2.5$ G (spectrum b of Figure 2). The spectrum of this radical appeared rapidly upon mixing (<130 s); its intensity decreased with time lasting for several minutes under our experimental conditions (an observed half-life of about 6 min). The WinSim program provided the best fit when the hydrogens and chlorine on the second ring made a contribution to the simulated spectrum (Table 1). These splitting constants are all very small; thus, their contribution is in essence only to the observed line width.

HRP/LPO with H_2O_2. Horseradish peroxidase (HRP) and lactoperoxidase (LPO) are the enzymes known to catalyze H_2O_2-dependent one-electron oxidations; these systems will oxidize hydroquinones to the corresponding $SQ^{\bullet -}$. When 2′-Cl-2,5-H_2Q was introduced into these systems, the spectra observed were consistent with the formation of 2′-Cl-2,5-$SQ^{\bullet -}$ (Figure 2c,d). When 3′-Cl-2,5-H_2Q or 4′-Cl-2,5-H_2Q was introduced, their corresponding $SQ^{\bullet -}$ radicals were observed (not shown). These spectra were identical (except for intensity) to those observed when their respective quinones were exposed to the HX/XO system. Thus, the same $SQ^{\bullet -}$ can be derived from either the hydroquinone or the quinone with appropriate one-electron oxidation or reduction.

Tyrosinase. Tyrosinase (TYR) is a copper-containing enzyme present in plant and animal tissues. It catalyzes the two-electron oxidation of *ortho*-hydroquinones (not *para*-hydroquinones) to their corresponding quinones (*29, 30*). In our reaction, tyrosinase will catalyze the oxidation of one molecule of PCB *ortho*-hydroquinone to its quinone with the reduction of 1/2 molecule of oxygen to form one H_2O (Scheme 1). This introduction of quinone will allow the formation of $SQ^{\bullet -}$ via the comproportionation of hydroquinone and quinone. In air-saturated buffer at pH 7.4, 100 μM *ortho*-hydroquinone 4′-Cl-3,4-H_2Q produced a small background EPR signal of 4′-Cl-3,4-$SQ^{\bullet -}$ (at the noise level), due to the slow oxidation of the hydroquinone (not shown). However, in the presence of TYR, a much stronger EPR spectrum of $SQ^{\bullet -}$ from 4′-Cl-3,4-H_2Q was observed (Figure 2e). When a *para*-hydroquinone was exposed to TYR, no increase in $SQ^{\bullet -}$ was observed (not shown). In the EPR experiments, if too much TYR was introduced into the incubation such that all of the hydroquinone was very rapidly oxidized to quinone, the EPR signal of $SQ^{\bullet -}$ was quite weak or below the limit of detection.

If reaction mixtures identical to those used for EPR were monitored for oxygen consumption, the predicted stoichiometric loss of oxygen was observed with *ortho*-hydroquinones, while no oxygen was lost with *para*-hydroquinones. These results demonstrate that *ortho*-hydroquinone-PCBs have additional mechanisms for radical formation as compared to *para*-hydroquinone PCBs.

Autoxidation in Aerobic Solutions. When the phenolic OH groups of hydroquinones ionize, the anions are prone to rapid autoxidation. Indeed, the semiquinone radical of hydroquinone was observed by EPR spectroscopy in the 1950s when it was introduced to oxygenated, alkaline media (*31*). We hypothesized that hydroquinone derivatives of PCBs would also undergo a parallel autoxidation reaction and generate corresponding PCB semiquinones (Scheme 2A). To examine this hypothesis, we introduced 2′-Cl-2,5-H_2Q to an alkaline environment (pH 10); we obtained the corresponding $SQ^{\bullet -}$ radical (Figure 2f and Table 1). It has been suggested that the generation of $SQ^{\bullet -}$ in alkaline solution is only the first stage of the autoxidation of dihydroxy phenols (*32–34*). The radical can continue to oxidize to quinone, and then, a comproportionation reaction will turn one molecule of hydroquinone and one molecule of quinone into two molecules of $SQ^{\bullet -}$ (Scheme 2B). Increasing the pH from 7 to 12 dramatically increased the concentration of the initially formed $SQ^{\bullet -}$; this is because high [OH^-] increases the rate of autoxidation of hydroquinone and decreases the rate of decay of $SQ^{\bullet -}$, principally by disproportionation (Scheme 1), which is dependent on $[H^+]^2$ (*35*).

Using the HX/XO system, we have shown above that PCB quinones can be reduced by one electron to corresponding PCB semiquinone radicals. In addition, H_2Q can be oxidized to form $SQ^{\bullet -}$; high pH can increase this rate. However, a most surprising observation is that 2′-Cl-2,5-Q in high pH solution also generates a strong $SQ^{\bullet -}$ signal (Figure 2g). To generate $SQ^{\bullet -}$ from Q, there must be a source of electrons. In this experiment, we observed that the EPR signal for the initial $SQ^{\bullet -}$ (≈1:3:3:1) radical gives way to a 1:2:1 spectrum, consistent with the formation of a secondary radical $SQ(II)^{\bullet -}$. A possible mechanism for the continued autoxidation PCB quinone is described in Scheme 2C. The evolution of the EPR spectrum from a ≈1:3:3:1 pattern to a 1:2:1 pattern indicates the loss of a hydrogen from the quinone ring (Figure 3). This suggests a base-catalyzed Michael addition of an

Table 1. Hyperfine splitting Constants from the Various PCB-SQ$^{\bullet-}$[a]

compd	2	3	4	5	6	2′	3′	4′	5′	6′	line width[b]
2′-Cl-2,5-Q	(OH)	2.2 (H)	2.4 (H)	(OH)	2.2 (H)	0.1 (Cl)	0.1 (H)	0.1 (H)	0.1 (H)	0.2 (H)	0.17
3′-Cl-2,5-Q	(OH)	2.1 (H)	2.5 (H)	(OH)	2.1 (H)	0.1 (H)	0.1 (Cl)	0.1 (H)	0.2 (H)	0.2 (H)	0.37
4′-Cl-2,5-Q	(OH)	2.1 (H)	2.5 (H)	(OH)	2.1 (H)	0.2 (H)	0.1 (H)	0.1 (Cl)	0.1 (H)	0.2 (H)	0.32
3′,4′-Cl-2,5-Q	(OH)	2.1 (H)	2.5 (H)	(OH)	2.1 (H)	0.1 (H)	0.17 (Cl)	0.1 (Cl)	0.1 (H)	0.3 (H)	0.32
2′-Cl-2,5-H_2Q	(OH)	2.2 (H)	2.5 (H)	(OH)	2.2 (H)	0.1 (Cl)	0.1 (H)	0.1 (H)	0.1 (H)	0.2 (H)	0.11
3′-Cl-2,5-H_2Q	(OH)	2.1 (H)	2.5 (H)	(OH)	2.1 (H)	0.1 (H)	0.1 (Cl)	0.2 (H)	0.2 (H)	0.3 (H)	0.09
4′-Cl-2,5-H_2Q	(OH)	2.1 (H)	2.5 (H)	(OH)	2.1 (H)	0.2 (H)	0.1 (H)	0.1 (Cl)	0.1 (H)	0.2 (H)	0.19
4′-Cl-2,3-H_2Q	(OH)	(OH)	0.5 (H)	3.9 (H)	3.2 (H)	0.1 (H)	0.1 (H)	0.1 (Cl)	0.1 (H)	0.1 (H)	0.10
3′,4′-Cl-2,3-H_2Q	(OH)	(OH)	0.6 (H)	3.8 (H)	3.3 (H)	0.1 (H)	0.1 (Cl)	0.1 (Cl)	0.1 (H)	0.1 (H)	0.14
4′-Cl-3,4-H_2Q	0.1 (H)	(OH)	(OH)	1.2 (H)	3.2 (H)	0.7 (H)	0.3 (H)	0.1 (Cl)	0.3 (H)	0.7 (H)	0.11
2′,5′-Cl-3,4-H_2Q	0.7 (H)	(OH)	(OH)	1.0 (H)	3.3 (H)	0.2 (Cl)	0.4 (H)	0.2 (H)	0.2 (Cl)	0.6 (H)	0.20
2′,3′-Cl-3,4-H_2Q	0.8 (H)	(OH)	(OH)	1.1 (H)	3.3 (H)	0.3 (Cl)	0.2 (Cl)	0.1 (H)	0.2 (H)	0.4 (H)	0.07

[a] These hyperfine splittings (in Gauss) are the results from simulations of the experimental spectra. Assignment of hyperfine splittings to particular hydrogens on the semiquinone ring followed examples of previously published work (*36–38*). On the secondary ring, we make no definite assignments. The numbering pattern is for the structure:

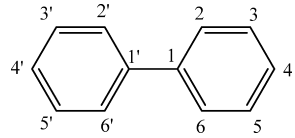

[b] In Gauss.

Scheme 2. Mechanisms for the Autoxidation of PCB Hydroquinone and Quinone To Generate SQ$^{\bullet-}$ and SQ(II)$^{\bullet-}$

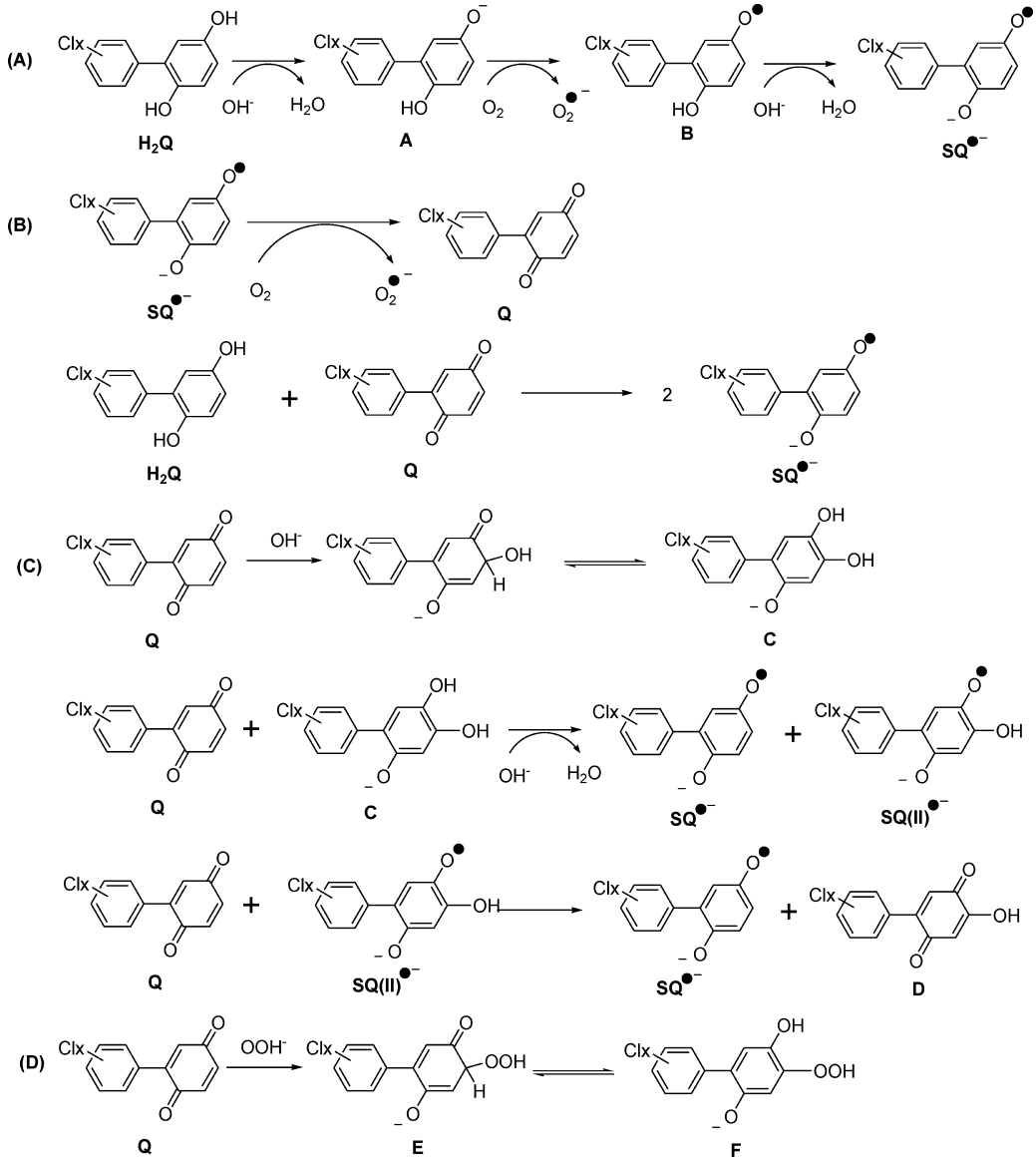

OH^- to the quinone ring (OH^- can in principle substitute for any of the three hydrogens on the quinone ring; only one possibility is shown) (Scheme 2C). When quinone is introduced to an alkaline solution, we initially see only the primary

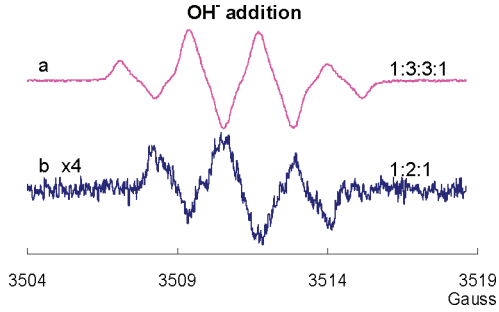

Figure 3. EPR spectra from dihydroxyl and trihydroxyl PCB: Changes in the EPR spectra of 2′-Cl-2,5-H_2Q after introduction of NaOH (15 μL of 5 M NaOH add into 2000 μL of 100 μM 2′-Cl-2,5-H_2Q in buffer): (a) before introduction of NaOH and (b) 5 min after the introduction of NaOH. The EPR modulation amplitude was 1 G.

radical, $SQ^{\bullet-}$; the secondary radical $SQ(II)^{\bullet-}$ is observed after some time has passed, indicating that the reaction is somewhat slow and a significant amount of the trihydroxy compound must be formed before the 1:2:1 spectrum can be observed. The addition of OH^- to the quinone ring provides the reducing equivalents to form the initial $SQ^{\bullet-}$ observed as well as $SQ(II)^{\bullet-}$ (Scheme 2C).

$SQ^{\bullet-}$ Via Comproportionation. To demonstrate that $SQ^{\bullet-}$ can be formed by the comproportionation reaction of H_2Q and Q, we examined by EPR solutions containing both species (Scheme 2B). We used quinhydrone, a charge transfer complex consisting of equal parts of hydroquinone interacting with benzoquinone through ring stacking, as a test system; a strong EPR spectrum for the benzosemiquinone radical was observed in neutral solution consistent with an equilibrium comproportionation reaction (spectrum not shown; it has the same characteristics as the spectrum of Figure 2a). When 2′-Cl-2,5-Q and 2′-Cl-2,5-H_2Q were mixed (1:1 ratio, 50 μM each) in neutral solution, the corresponding $SQ^{\bullet-}$ radical was observed by EPR (Figure 2h). When the ratio of H_2Q:Q was varied over the range of 1:9 to 9:1 (keeping $[H_2Q] + [Q] =$ 100 μM), $SQ^{\bullet-}$ was observed at all ratios with approximately the same intensity. This is consistent with comproportionation and disproportionation reactions achieving equilibrium rapidly, on the time scale of the EPR observations, with an accompanying autoxidation reaction removing the radical. As expected, the intensity of the EPR signal increased with increasing pH. At high pH, the hydroquinone will ionize, leading to a more rapid autoxidation; in addition, the disproportionation reaction is slowed, as protons are needed, thus a higher EPR signal intensity.

Characterization of $SQ^{\bullet-}$ Generated from a Wide Range of Oxygenated PCBs. Because semiquinone radicals are more stable in alkaline solution, we generated a series of PCB semiquinone radicals at pH 10 to investigate the influence of the chemical structure on the EPR spectra (Figure 4). Here, we focus on the initially formed, primary radicals that are observed upon raising the pH to 10.

The EPR spectra of the $SQ^{\bullet-}$ generated from different x_n' -Cl-2,5-Q and x_n'-Cl-2,5-H_2Q are quite similar (Figure 4A,B); starting with either the quinone or the hydroquinone of a specific x_n' -Cl-2,5-Q, the same semiquinone spectrum was observed. Hyperfine splitting constants, derived from simulation (Table 1), showed three nearly identical hydrogens, which yield a 1:3:3:1 four-line spectrum. These results show that the primary interactions are with the hydrogens on the semiquinone ring; the other ring provides no unique splittings, perhaps only contributing to the line width.

There are two different families of PCB *ortho*-hydroquinones, 2,3-H_2Q and 3,4-H_2Q. When oxidized to their corresponding $SQ^{\bullet-}$, each member of a family produced a similar EPR spectral pattern (Figure 4C,D and Table 1). Successful simulations of spectra from 2,5-$SQ^{\bullet-}$ or 2,3-$SQ^{\bullet-}$ did not require any contributions of hyperfine splittings from the other phenyl ring. However, for the 3,4-$SQ^{\bullet-}$ (Figure 4D), hyperfine splittings from the second phenyl ring contributed markedly. Definitive assignments of hyperfine splittings to specific H or Cl atoms from the second phenyl ring (the phenyl ring with Cl) have not been made (Table 1). We have used the literature (*36–38*) to guide our assignment of the hyperfine splitting constants for the hydrogens on the semiquinone ring. The simulation results are consistent with low spin density on the secondary ring. However, the x_n'-Cl-3,4-$SQ^{\bullet-}$ radicals show considerable spin density on the secondary ring, especially 4′-Cl-3,4-$SQ^{\bullet-}$.

Spin Trapping with DMPO. Semiquinones can transfer an electron to oxygen generating the superoxide radical (*18, 39*). Superoxide can play a key role in the generation of oxidative damage under various pathophysiological conditions. However, $O_2^{\bullet-}$ is very short-lived, and in most cases, the sensitivity of EPR spectroscopy is insufficient for direct detection. Thus, we used EPR spin trapping to probe for the formation of superoxide radicals (*40–42*). A spin trap reacts with short-lived radicals to form much longer-lived spin adducts that accumulate to a level detectable by EPR.

In Figure 5, spectrum "a" is a control demonstrating the absence of artifactual signals from DMPO. Spectrum "b" represents the typical DMPO/$^{\bullet}$OOH spin adduct generated from HX/XO system and trapped by DMPO; some DMPO/$HO^{\bullet}$ spin adduct is also present. When 2′-Cl-2,5-Q was added to DMPO in neutral solution, both $SQ^{\bullet-}$ and DMPO/$HO^{\bullet}$ were detected (Figure 5c). If SOD was included, there was no significant change in the intensity of the spectrum of $SQ^{\bullet-}$ (spectrum "d"), but the signal of the DMPO/$HO^{\bullet}$ radical increased. Because no evidence for DMPO/$^{\bullet}$OOH radical was observed in "c" and SOD did not decrease the DMPO/$HO^{\bullet}$ signal, there appears to be no significant superoxide formation from 2′-Cl-2,5-Q.

When 2′-Cl-2,5-H_2Q was substituted for 2′-Cl-2,5-Q, the addition of SOD stimulated the generation of $SQ^{\bullet-}$ (Figure 5e,f); the intensity of the $SQ^{\bullet-}$ spectrum increased over time, reached a steady state, and then decreased (data not shown). Cat had no effect on the generation of $SQ^{\bullet-}$ or DMPO/$HO^{\bullet}$ radical (not shown). These observations indicate that generation of superoxide from $SQ^{\bullet-}$, reaction 1, is not kinetically or thermodynamically favorable.

$$SQ^{\bullet-} + O_2 \rightleftharpoons O_2^{\bullet-} + Q \qquad (1)$$

The equilibrium for this reaction lies far to the left. Using benzoquinone and various substituted quinones as references, the rate constant for the forward reaction will be approximately 10^4-10^5 M^{-1} s^{-1}, while the rate constant for the reverse reaction is on the order of 10^9 M^{-1} s^{-1} (*18, 43, 44*). This rapid back reaction explains why our spin trapping experiment cannot detect superoxide formation.

SOD Catalyzes the Autoxidation of Hydroquinone as Seen by UV Spectroscopy. The increase in $[SQ^{\bullet-}]$ observed in Figure 5f suggests that SOD can catalyze the autoxidation of 2′-Cl-2,5-H_2Q to 2′-Cl-2,5-Q. To observe if the rate of formation of 2′-Cl-2,5-Q increases when SOD is added to a near-neutral solution of 2′-Cl-2,5-H_2Q, we used UV spectroscopy to follow the rate of formation of 2′-Cl-2,5-Q. In the absence of SOD, the autoxidation of 2′-Cl-2,5-H_2Q (100

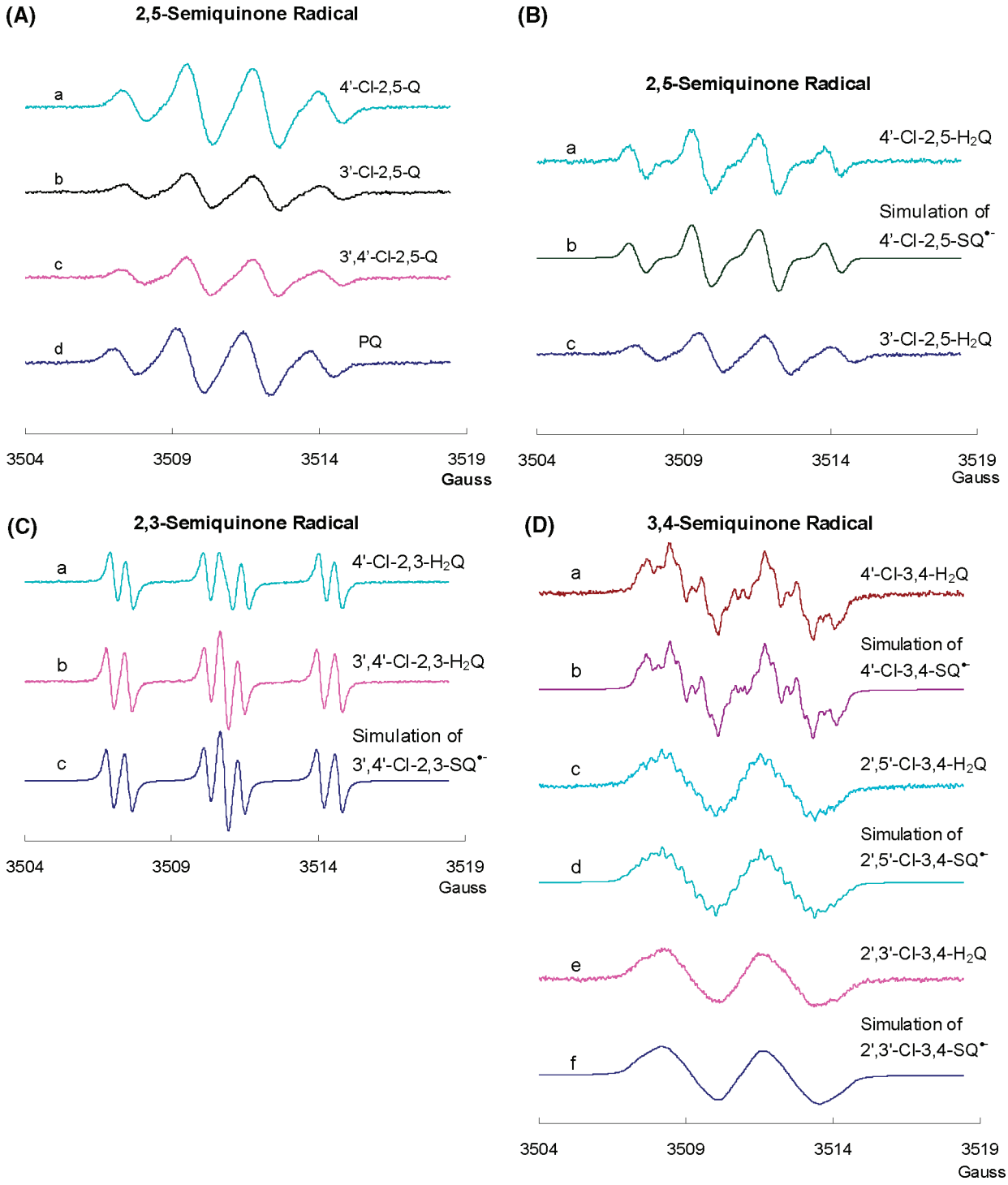

Figure 4. Semiquinone radical generated from PCB with different substitution patterns at pH 10 and computer simulations. Hyperfine splittings and spectral line widths derived by simulation of experimental spectra are presented in Table 1. (A) Semiquinone radicals generated from different 2,5-Q at pH 10: (a) $SQ^{\bullet-}$ generated from 4′-Cl-2,5-Q; (b) $SQ^{\bullet-}$ generated from 3′-Cl-2,5-Q; (c) $SQ^{\bullet-}$ generated from 3′, 4′-Cl-2,5-Q; and (d) $SQ^{\bullet-}$ generated from PQ. (B) Semiquinone radicals generated from different 2,5-H_2Q at pH 10: (a) $SQ^{\bullet-}$ generated from 4′-Cl-2,5-H_2Q; (b) simulation of 4′-Cl-2,5-$SQ^{\bullet-}$; and (c) $SQ^{\bullet-}$ generated from 3′-Cl-2,5-H_2Q. (C) Semiquinone radicals generated from different 2,3-H_2Q at pH 10: (a) $SQ^{\bullet-}$ generated from 4′-Cl-2,3-H_2Q; (b) $SQ^{\bullet-}$ generated from 3′,4′-Cl-2,3-H_2Q; and (c) simulation of 3′,4′-Cl-2,3- $SQ^{\bullet-}$. (D) Semiquinone radicals generated from different 3,4-H_2Q at pH 10: (a) $SQ^{\bullet-}$ generated from 4′-Cl-3,4-H_2Q; (b) simulation of 4′-Cl-3,4-$SQ^{\bullet-}$; (c) $SQ^{\bullet-}$ generated from 2′,5′-Cl-3,4-H_2Q; (d) simulation of 2′,5′-Cl-3,4-$SQ^{\bullet-}$; (e) $SQ^{\bullet-}$ generated from 2′,3′-Cl-3,4-H_2Q; and (f) simulation of 2′,3′-Cl-3,4-$SQ^{\bullet-}$. All experimental spectra were collected using a 0.1 G modulation amplitude.

μM) to quinone is relatively slow (Figure 6a,b). When SOD is present at time zero, there is no change in the initial rate of autoxidation; however, after about 10 min or so, autoxidation accelerates (Figure 6c). If a trace of 2′-Cl-2,5-Q (1 μM) is introduced at time zero along with SOD, there is no lag time for a much more rapid rate of autoxidation. These observations are parallel to those observed by Eyer in a study of hydroquinone autoxidation (*44*); this same process appears to hold with coenzyme Q semiquinone radical in mitochondria with changes in MnSOD (*45*). Superoxide is formed by reaction 1; however, the equilibrium lies far to the left. SOD pulls this equilibrium by removing superoxide before it enters the back reaction due to its very rapid dismutation of superoxide, reaction 2.

$$2H^+ + 2O_2^{\bullet -} \xrightarrow{SOD} O_2 + H_2O_2 \quad (2)$$

In the experiment of Figure 6c, the rate of autoxidation remains low until significant 2′-Cl-2,5-Q is generated, allowing for the comproportionation reaction of 2′-Cl-2,5-Q with 2′-Cl-2,5-H_2Q to form $SQ^{\bullet -}$, reaction 3. However, if a trace of 2′-Cl-2,5-Q is introduced at time zero (Figure 6d), no lag time is observed because all of the ingredients are present to make significant $SQ^{\bullet -}$.

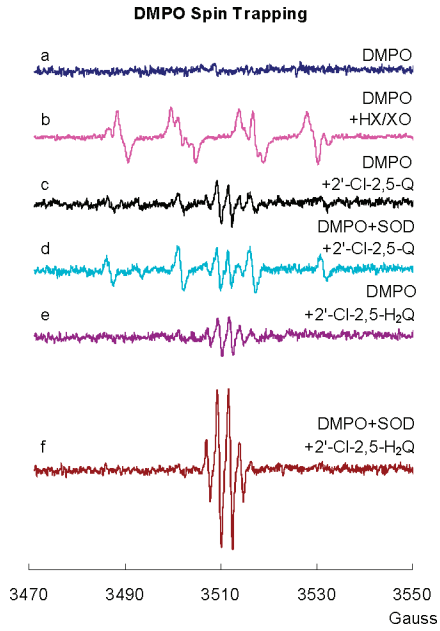

Figure 5. Spin trapping with DMPO indicates that superoxide formation is below the limit of detection. (a) EPR spectrum by DMPO (50 mM) in PBS with DETAPAC (250 μM); (b) superoxide and hydroxyl adducts of DMPO (50 mM) generated with HX/XO at pH 7.4 (a^N = 14.1 G, a^H = 11.3 G with an additional hydrogen splitting of 1.3 G for DMPO/$^{\bullet}$OOH, and $a^N = a^H$ = 14.9 G for DMPO/$^{\bullet}$OH); (c) spectrum generated from 2′-Cl-2,5-Q (1 mM) and DMPO (100 mM) at pH 7.4; (d) spectrum generated from 2′-Cl-2,5-Q (1 mM), DMPO (100 mM), and 500 U SOD/mL at pH 7.4; (e) spectrum generated from 2′-Cl-2,5- H_2Q (1 mM) and DMPO (100 mM) at pH 7.4; and (f) spectrum generated from 2′-Cl-2,5-H_2Q (1 mM), DMPO (100 mM), and 500 U SOD/mL at pH 7.4. All experimental spectra were collected using a 1.0 G modulation amplitude.

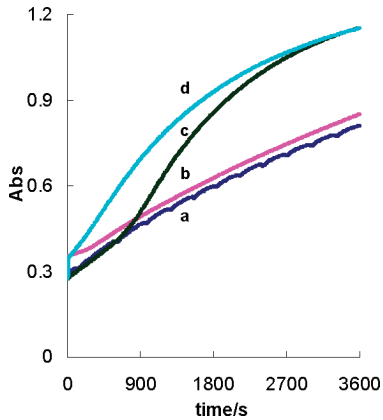

Figure 6. SOD accelerates the autoxidation of hydroquinone. The formation of 2′-Cl-2,5-Q during the autoxidation of 2′-Cl-2,5-H_2Q (0.1 mM) was followed at 249 nm. (a) 2′-Cl-2,5-H_2Q (0.1 mM); (b) 2′-Cl-2,5-H_2Q (0.1 mM) mixed with 2′-Cl-2,5-Q (1 μM); (c) 2′-Cl-2,5-H_2Q (0.1 mM) with 100 U/mL SOD; and (d) 2′-Cl-2,5-H_2Q (0.1 mM) mixed with 2′-Cl-2,5-Q (1 μM) plus 100 U/mL SOD.

$$H_2Q + Q \rightleftharpoons 2SQ^{\bullet -} + 2H^+ \quad (3)$$

These observations suggest that oxygen will be consumed in the autoxidation reaction, giving rise to the formation of H_2O_2, the net reaction being

$$H_2Q + O_2 \rightarrow H_2O_2 + Q \quad (4)$$

Oxygen Consumption. Oxygen Uptake at Near-Neutral pH. If SOD accelerates the rate of oxidation of 2′-Cl-2,5-H_2Q as seen by formation of quinone, then the rate of oxygen consumption should also increase. Indeed, when 2′-Cl-2,5-H_2Q (500 μM) was introduced into pH 7.4 PBS, the rate of oxygen consumption paralleled all of the results of Figure 6 (data not shown). The introduction of Cat to a partially oxidized solution of 2′-Cl-2,5-H_2Q demonstrated that nearly all of the oxygen consumed was present as H_2O_2. These observations support reactions 1–4 as being operative in this system.

Oxygen Uptake in Alkaline pH Solutions. Autoxidation of 2′-Cl-2,5-H_2Q in alkaline pH is accelerated due to ionization of the phenolic hydroxyls and subsequent one-electron oxidation to 2′-Cl-2,5-$SQ^{\bullet -}$, followed by loss of a second electron yielding 2′-Cl-2,5-Q. One might predict that 1 equiv of H_2Q would consume 1 equiv of dioxygen, yielding 1 equiv of H_2O_2 (reaction 4). Interestingly, the amount of oxygen consumed is a function of pH (Figure 7). We observed a sharp increase in the amount of oxygen consumed as the pH was increased from pH 8 to pH 13. At higher pH values, we observed that H_2Q consumed almost 2 equiv of oxygen, rather than the 1 equiv anticipated; unexpectedly, we observed that the quinone also consumed oxygen in a pH-dependent manner. The amounts of oxygen consumed by H_2Q and Q paralleled each other; the quinone form always consumed one-half equiv less oxygen than H_2Q at a particular pH. These observations are consistent with oxidation of hydroquinone to quinone, followed by the nucleophilic addition of OH^- to the quinone forming a trihydroxy compound that can be oxidized in the high pH environment (Scheme 2C). When starting with the quinone, there would be no initial oxidation; thus, less oxygen would be consumed.

The rate of consumption of oxygen is dramatically increased upon initiating a pH jump of a near-neutral solution of the oxygenated PCBs that we examined (Figure 7). If reaction 4 is operative, then H_2O_2 should be formed. We investigated this possible formation of H_2O_2 using 2′-Cl-2,5-H_2Q and 2′-Cl-2,5-

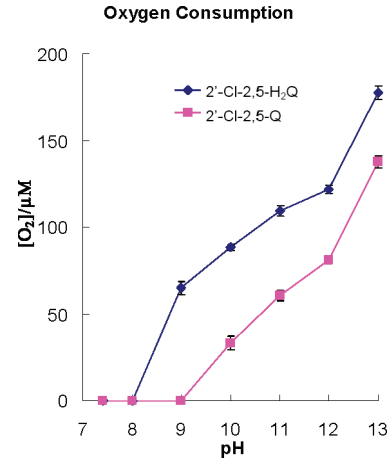

Figure 7. Oxygen consumption of PCB hydroquinone and quinone in different pH solutions. 2′-Cl-2,5-H_2Q (100 μM) or 2′-Cl-2,5-Q (100 μM) was introduced into the closed chamber of the YSI Biological Oxygen monitor containing solutions having different pH values. The data points are the means of three determinations; standard errors are in general smaller than the symbols used to present the data.

Table 2. Oxygen Uptake and Changes in [H_2O_2] upon Oxidation of 2′-Cl-2,5-H_2Q or 2′-Cl-2,5-Q by Increasing the pH

	change in oxygen concentration (μM)[a,b]				
additions	exp 1	exp 2	exp 3	exp 4	exp 5
2′-Cl-2,5-H_2Q (100 μM)[c]	0[d]	0	0	0	0
H_2O_2 (100 μM)	[e]		0		0
NaOH[f]		−170		−170	−90
H_2O_2 (100 μM)				0	
Cat (150 U/mL)	0	+<5	+50	+50	+30
expected with Cat[g]	0	+50	+50	+100	+100

	change in oxygen concentration (μM)[a,b]				
additions	exp 6	exp 7	exp 8	exp 9	exp 10
2′-Cl-2,5-Q (100 μM)	0	0	0	0	0
H_2O_2 (100 μM)			0		0
NaOH[f]		−70		−70	−50
H_2O_2 (100 μM)				0	
Cat (150 U/mL)	0	+<5	+50	+50	+5
expected with Cat[g]	0	+35	+50	+50	+50

[a] Each experiment was done at least three times. Variations between experiments are on the order of 10%. [b] Each entry represents the change in oxygen concentration after the addition. The additions were made sequentially as shown down column 1. [c] In PBS, pH 7.4. [d] The actual loss of oxygen is less than or on the order of the drift of the instrument, which typically is less than 5 μM per 15 min. [e] A blank cell indicates that there was no addition of this reagent and thus no change in [O_2]. [f] The addition of 20 μL of 5 M NaOH into 2 mL of buffer increases the pH of solution to over 12. [g] Expected return of oxygen assuming that the only important reaction upon introduction of NaOH is reaction 2 when hydroquinone is reactant; if quinone is the reactant, the expected return of oxygen assumes no reaction between the quinone and the H_2O_2.

Q. Cat disproportionates $2H_2O_2$ into $2H_2O$ and $1O_2$; thus, it can be used as a tool to examine the stoichiometry of the reduction O_2 to H_2O_2. In near-neutral solution, little or no oxygen was consumed after introduction of 2′-Cl-2,5-H_2Q (Table 2, exp 1). However, if the pH is increased to ≈12 by the addition of NaOH, a rapid loss of oxygen occurs (−170 μM) (Table 2, exp 2). If reaction 4 holds, we would have expected to lose only 100 μM O_2. These observations are consistent with Figure 7 and the reactions outlined in Scheme 2C. Most surprising was our observation that upon introduction of Cat, little if any oxygen returned, indicating that there was no hydrogen peroxide in the system. (Although high pH inactivates enzymes, this high pH did not inactivate Cat in the short time frame of an experiment; data not shown.)

To determine if the hydroquinone reacts directly with H_2O_2, we introduced 100 μM H_2O_2 into a neutral solution of 100 μM 2′-Cl-2,5-H_2Q. After 15 min, all of the H_2O_2 was still present as the introduction of Cat saw the return of 50 μM O_2 (Table 2, exp 3). Thus, there is no rapid direct reaction of hydroquinone with H_2O_2. In exp 4, we introduced H_2O_2 after the reactions initiated by the pH jump were complete. The addition of Cat resulted in the return of 50 μM O_2, demonstrating that there was no rapid direct reaction of H_2O_2 with the oxidation products of 2′-Cl-2,5-H_2Q. Interestingly, the introduction of H_2O_2 before the pH jump reduced oxygen consumption (−170 to −90 μM; Table 2, exp 5); Cat returned only 30 μM oxygen, indicating that some of the H_2O_2 was lost. Experiments 1−5 of Table 2 indicate that H_2O_2 must be reacting with intermediates in the oxidation reactions of 2′-Cl-2,5-H_2Q.

Hydrogen peroxide has been shown to react with benzoquinone (*46*) and chlorinated benzoquinone (*47*). Experiments 6−10 of Table 2 examine the possible reaction of H_2O_2 with a typical PCB-quinone, 2′-Cl-2,5-Q. At near-neutral pH, there was no apparent reaction of H_2O_2 with 2′-Cl-2,5-Q (exp 8). However, experiments 7 and 10 show a considerable loss of H_2O_2 upon a pH jump. An explanation for this observation is that in pH 12 solution, some H_2O_2 will be deprotonated (pK_1 for H_2O_2 to form OOH^- is 11.7, *48*). The peroxide anion is a powerful nucleophile, much more reactive than hydroxide anion (*47*). It will react with PCB quinone, similar to OH^-; however, the reaction will likely be much faster (Scheme 2D). Thus, experiments 7 and 10 in Table 2 with 2′-Cl-2,5-Q are consistent with a rapid nucleophilic addition reaction of H_2O_2, via OOH^-, to the quinone.

Conclusions

In this work, we have demonstrated the following:

1. The same semiquinone radical is produced when a PCB-hydroquinone undergoes a one-electron oxidization or the quinone form undergoes a one-electron reduction. This can be accomplished many different ways, including the following:
   (a) Xanthine oxidase can reduce quinone PCBs to the corresponding $SQ^{\bullet-}$.
   (b) The heme-containing peroxidases (horseradish and lactoperoxidase) can oxidize hydroquinone PCBs to the corresponding $SQ^{\bullet-}$.
   (c) Tyrosinase acting on PCB *ortho*-hydroquinones leads to formation of $SQ^{\bullet-}$.
   (d) $SQ^{\bullet-}$ is formed rapidly when hydroquinone-PCBs undergo air oxidation in high pH buffer (≈>pH 8).
   (e) Quinone-PCBs in high pH buffer can also form $SQ^{\bullet-}$.
   (f) Mixtures of PCB-quinone and hydroquinone form $SQ^{\bullet-}$ via a comproportionation reaction.
2. The EPR spectra of semiquinone radicals produced from structurally similar PCB hydroquinones and quinones had similar spectral patterns as characterized by hyperfine splittings.
3. The production of superoxide radicals could not be observed using DMPO as a spin trapping agent due to the rapid reaction of superoxide with quinone; however, SOD accelerates the autoxidation of hydroquinone indicating a role for superoxide.
4. At higher pH, hydroxide anion can add to the quinone ring of a PCB-quinone, leading to the formation of a new hydroquinone and rupture of the quinone ring.
5. Using oxygen consumption at higher pH, the autoxidation of both hydroquinone and quinone consumed oxygen—this oxygen consumption could be greater than the 1:1 stoichiometry predicted by reaction 2.
6. H_2O_2 does not accumulate when a PCB-hydroquinone autoxidizes at high pH; H_2O_2 appears to react with intermediates formed during the oxidation process.
7. H_2O_2 accumulates when SOD is present in an autoxidizing PCB-hydroquinone solution at near-neutral pH; without

SOD, the reaction is too slow to observe any loss of O_2 or accumulation of H_2O_2.

Acknowledgment. This project was supported by Grant Numbers P42ES013661, P30ES05605, and K25ES012475 (H.-J.L.) from the National Institute of Environmental Health Sciences and R01GM073929 from the National Institute of General Medical Sciences. The content is solely the responsibility of the authors and does not necessarily represent the official views of the NIMGS or the NIH. The University of Iowa ESR Facility provided invaluable support.

References

(1) Safe, S. H. (1994) Polychlorinated biphenyls (PCBs): Environmental impact, biochemical and toxic responses, and implications for risk assessment. *Crit. Rev. Toxicol. 24*, 87–149.
(2) Silberhorn, E. M., Glauert, H. P., and Robertson, L. W. (1990) Carcinogenicity of polyhalogenated biphenyls: PCBs and PBBs. *Crit. Rev. Toxicol. 20*, 440–496.
(3) Robertson, L. W., and Hansen, L. G., Eds. (2001) *PCBs: Recent Advances in the Environmental Toxicology and Health Effects*, The University Press of Kentucky, Lexington, KY.
(4) Hansen, L. G. (1998) Stepping backward to improve assessment of PCB congener toxicities. *Environ. Health Perspect. 106*, 171–189.
(5) Cogliano, V. J. (1998) Assessing the cancer risk from environmental PCBs. *Environ. Health Perspect. 106*, 317–323.
(6) Dobson, S., and van Esch, G. J. (1993) Environmental Health Criteria 140: Polychlorinated Biphenyls and Terphenyls, 2nd ed., World Health Organization, Geneva. Also available at http://www.inchem.org/documents/ehc/ehc/ehc140.htm.
(7) Kennedy, M. W., Carpentier, N. K., Dymerski, P. P., Adams, S. M., and Kaminsky, L. S. (1980) Metabolism of monochlorobiphenyls by hepatic microsomal cytochrome P-450. *Biochem. Pharmacol. 29*, 727–736.
(8) Kennedy, M. W., Carpentier, N. K., Dymerski, P. P., and Kaminsky, L. S. (1981) Metabolism of dichlorobiphenyls by hepatic microsomal cytochrome P-450. *Biochem. Pharmacol. 30*, 577–588.
(9) Kaminsky, L. S., Kennedy, M. W., Adams, S. M., and Guengerich, F. P. (1981) Metabolism of dichlorobiphenyls by highly purified isozymes of rat liver cytochrome P-450. *Biochemistry 20*, 7379–7384.
(10) McLean, M. R., Bauer, U., Amaro, A. R., and Robertson, L. W. (1996) Identification of catechol and hydroquinone metabolites of 4-monochlorobiphenyl. *Chem. Res. Toxicol. 9*, 158–164.
(11) Bachur, N. R., Gordon, S. L., and Gee, M. V. (1978) A general mechanism for microsomal activation of quinone anticancer agents to free radicals. *Cancer Res. 38*, 1745–1750.
(12) Amaro, A. R., Oakley, G. G., Bauer, U., Spielmann, H. P., and Robertson, L. W. (1996) Metabolic activation of PCBs to quinones: reactivity toward nitrogen and sulfur nucleophiles and influence of superoxide dismutase. *Chem. Res. Toxicol. 9*, 623–629.
(13) McLean, M. R., Robertson, L. W., and Gupta, R. C. (1996) Detection of PCB adducts by the ^{32}P-postlabeling technique. *Chem. Res. Toxicol. 9*, 165–171.
(14) Oakley, G. G., Devanaboyina, U., Robertson, L. W., and Gupta, R. C. (1996) Oxidative DNA damage induced by activation of polychlorinated biphenyls (PCBs): Implications for PCB-induced oxidative stress in breast cancer. *Chem. Res. Toxicol. 9*, 1285–1292.
(15) Oakley, G. G., Robertson, L. W., and Gupta, R. C. (1996) Analysis of polychlorinated biphenyl-DNA adducts by ^{32}P-postlabeling. *Carcinogenesis 17*, 109–114.
(16) Bolton, J. L., Trush, M. A., Penning, T. M., Dryhurst, G., and Monks, T. J. (2000) Role of quinones in toxicology. *Chem. Res. Toxicol. 13*, 135–160.
(17) Monks, T. J., and Jones, D. C. (2002) The metabolism and toxicity of quinones, quinoneimines, quinone methides, and quinone-thioethers. *Curr. Drug Metab. 3*, 425–438.
(18) O'Brien, P. J. (1991) Molecular mechanisms of quinone cytotoxicity. *Chem.-Biol. Interact. 80*, 1–41.
(19) Lehmler, H.-J., and Robertson, L. W. (2001) Synthesis of polychlorinated biphenyls (PCBs) using the Suzuki-coupling. *Chemosphere 45*, 137–143.
(20) Lehmler, H.-J., and Robertson, L. W. (2001) Synthesis of hydroxylated PCB metabolites with the Suzuki-coupling. *Chemosphere 45*, 1119–1127.
(21) Kania-Korwel, I., Sean, P., Robertson, L. W., and Lehmler, H.-J. (2004) Synthesis of polychlorinated biphenyls and their metabolites with a modified Suzuki-coupling. *Chemosphere 56*, 735–744.
(22) Duling, D. R. (1994) Simulation of multiple isotropic spin-trap EPR spectra. *J. Magn. Res. Ser. B 104*, 105–110.
(23) Bachur, N. R., Gordon, S. L., Gee, M. V., and Kon, H. (1979) NADPH cytochrome P-450 reductase activation of quinone anticancer agents to free radicals. *Proc. Natl. Acad. Sci. U.S.A. 76*, 954–957.
(24) Iyanagi, T., and Yamazaki, I. (1969) One-electron transfer reactions in biochemical systems. III. One-electron reduction of quinones by microsomal flavin enzymes. *Biochim. Biophys. Acta 172*, 370–381.
(25) Plancherel, D., and Zelewsky, A. V. (1982) Proton-triggered complex formation: Radical complexes of *o*-benzosemiquinone, dopa, dopamine and adrenaline formed by electron transfer reaction from excited tris (2,2′-bipyridy1) ruthenium(II). *Helv. Chim. Acta 65*, 1929–1940.
(26) Kalyanaraman, B., Morehouse, K. M., and Mason, R. P. (1991) An electron paramagnetic resonance study of the interactions between the adriamycin semiquinone, hydrogen peroxide, iron-chelators, and radical scavengers. *Arch. Biochem. Biophys. 286*, 164–170.
(27) Yamazaki, I., and Piette, L. H. (1965) Electron paramagnetic resonance of undissociated *p*-benzosemiquinones. *J. Am. Chem. Soc. 87*, 986–990.
(28) Pedersen, J. A. (2002) On the application of electron paramagnetic resonance in the study of naturally occurring quinones and quinols. *Spectrochim. Acta, Part A 58*, 1257–1270.
(29) Korytowski, W., Sarna, T., Kalyanaraman, B., and Sealy, R. C. (1987) Tyrosinase-catalyzed oxidation of dopa and related catechol(amine)s: A kinetic electron spin resonance investigation using spin-stabilization and spin label oximetry. *Biochim. Biophys. Acta 924*, 383–392.
(30) Ferrari, R. P., Laurenti, E., Ghibaudi, E. M., and Casella, L. (1997) Tyrosinase-catecholic substrates in Vitro model: Kinetic studies on the o-quinone/o-semiquinone radical formation. *J. Inorg. Biochem. 68*, 61–69.
(31) Venkataraman, B., and Fraenkel, G. K. (1955) Proton hyperfine interactions in paramagnetic resonance of semiquinones. *J. Am. Chem. Soc. 77*, 2707–2713.
(32) Ashworth, P., and Dixon, W. T. (1972) Secondary radicals in the autoxidation of hydroquinones and quinones. *J. Chem. Soc., Perkin Trans. 2* 1130–1133.
(33) Stone, T. J., and Waters, W. A. (1965) Aryloxy-radicals. Part IV. Electron spin resonance spectra of some *ortho*-monobenzosemiquinones and secondary radicals derived therefrom. *J. Chem. Soc.* 1488–1494.
(34) Ashworth, P., and Dixon, W. T. (1971) Secondary radicals in the autoxidation of hydroquinones. *J. Chem. Soc. D* 1150–1152.
(35) Roginsky, V., and Barsukova, T. (2000) Kinetics of oxidation of hydroquinones by molecular oxygen. Effect of superoxide dismutase. *J. Chem. Soc., Perkin Trans. 2* 1575–1582.
(36) Pedersen, J. A. (1973) Electron spin resonance studies of oxidative processes of quinones and hydroquinones in alkaline solution; formation of primary and secondary semiquinone radicals. *J. Chem. Soc., Perkin Trans. 2* 424–431.
(37) Ashworth, P., and Dixon, W. T. (1972) Electron spin resonance spectra of radicals derived from arylhydroquinones. *J. Chem. Soc., Perkin Trans. 2* 2264–2267.
(38) Venkataraman, B., Segal, B. G., and Fraenkel, G. K. (1959) Paramagnetic resonance of methyl- and chloro-substituted *p*-benzosemiquinones. *J. Chem. Phys. 30*, 1006–1016.
(39) Francesco, A. M. D., Ward, T. H., and Butler, J. (2004) Diaziridinylbenzoquinones. *Methods Enzymol. 382*, 174–193.
(40) Buettner, G. R. (1993) The spin trapping of superoxide and hydroxyl free radicals with DMPO (5,5-dimethylpyrroline-*N*-oxide): More about iron. *Free Radical Res. Commun. 19* (Suppl. 1), S79−S87.
(41) Pou, S., Hassett, D. J., Britigan, B. E., Cohen, M. S., and Rosen, G. M. (1989) Problems associated with spin trapping oxygen-centered free radicals in biological systems. *Anal. Biochem. 177*, 1–6.
(42) Buettner, G. R., and Mason, R. P. (1990) Spin-trapping methods for detecting oxygen-derived radical formation in vitro and in vivo. *Methods Enzymol. 186*, 127–133.
(43) Roginsky, V. A., Pisarenko, L. M., Bors, W., and Michel, C. (1999) The kinetics and thermodynamics of quinine−semiquinone−hydroquinone systems under physiological conditions. *J. Chem. Soc., Perkin Trans. 2* 871–876.
(44) Eyer, P. (1991) Effects of superoxide dismutase on the autoxidation of 1,4-hydroquinone. *Chem.-Biol. Interact. 80*, 159–176.
(45) Buettner, G. R., Ng, C. F., Wang, W., Rodgers, V. G. J., and Schafer, F. Q. (2006) A new paradigm: Manganese superoxide dismutase influences the production of H_2O_2 in cells and thereby their biological state. *Free Radical Biol. Med. 41*, 1338–1350.
(46) Brunmark, A. (1989) Formation of electronically excited states during the interaction of benzoquinone with hydrogen peroxide. *J. Biolumin. Chemilumine. 4*, 219–225.
(47) Zhu, B. Z., Kalyanaraman, B., and Jiang, G. B. (2007) Molecular mechanism for metal-independent production of hydroxyl radicals by hydrogen peroxide and halogenated quinones. *Proc. Natl. Acad. Sci. U.S.A. 104*, 17575–17578.
(48) Curci, R., and Edwards, J. O. (1992) Activation of hydrogen peroxide by organic compounds. In *Catalytic Oxidations with Hydrogen Peroxide as Oxidant* (Strukul, G., Ed.) In the series Catalysis by Metal Complexes, Vol. 9, Chapter 2, Springer-Verlag LLC, New York.

TX8000175